International Journal of GEOMATE, April, 2026 Vol.30, Issue 140, pp.156-163
ISSN: 2186-2982 (P), 2186-2990 (O), Japan, DOI: https://doi.org/10.21660/2026.140.5445
Geotechnique, Construction Materials and Environment

BOLTED SHEAR CONNECTORS IN ULTRA HIGH PERFORMANCE CONCRETE COMPOSITE SLABS WITH STEEL DECK: A NUMERICAL INVESTIGATION

Hieu Nghia Hoang, *Quoc Anh Vu[2] and Viet Chinh Mai[3]

[1]Faculty of Technology and Engineering, Hai Phong University, Hai Phong, Viet Nam
[2]Faculty of Civil Engineering, Hanoi Architectural University, Vietnam
[3]Institute of Construction Technology, Le Quy Don Technical University, Hanoi, Vietnam

*Corresponding Author, Received: 22 Jan. 2026, Revised: 10 March 2026, Accepted: 24 March 2026

ABSTRACT: This study presents a comprehensive three-dimensional nonlinear finite element (FE) model developed in ABAQUS to investigate the behavior of bolted shear connectors embedded in Ultra high performance concrete (UHPC) composite slabs with steel decking. Material nonlinearity was modelled using ductile and shear damage criteria for steel material and the Concrete Damaged Plasticity (CDP) model for UHPC. Model accuracy was validated against experimental push-out tests from the literature, showing a good agreement in load-slip response and peak load. Following validation, an extensive parametric study was conducted to assess the influence of UHPC compressive strength, connector diameter, and reinforcement configuration. Increasing the UHPC compressive strength from 120 MPa to 180 MPa increased the shear capacity from 96.8 kN to 133.4 kN, corresponding to an enhancement of 1.38 times. Among all parameters, the connector diameter exhibited the most pronounced influence, with an increase of 1.52 times. The results is mainly due to enhanced confinement and bearing resistance around the connector. In contrast, modifications to the reinforcement cage such as using double reinforcement layers or reducing bar spacing, resulted in only marginal (1-3%) improvements. The findings provide valuable insights into shear transfer mechanisms in steel-UHPC composite systems and offer a validated numerical framework for optimizing connector design.

Keywords: Ultra High Performance Concrete, Bolted shear connectors, Simulation model, Composite slabs

1. INTRODUCTION

Steel-concrete composite structures have been extensively adopted in bridges and buildings because they combine the high compressive strength of concrete with the excellent tensile performance of steel members [1-3]. This synergy allows for lighter, stronger, and more economical structures with improved stiffness and ductility. A critical component in achieving full composite action is the shear connector, which transfers longitudinal shear forces across the steel–concrete interface and prevents slip between the two materials. The most commonly used type is the welded headed stud, favored for its simplicity and reliability in both static and fatigue conditions. Recently, bolted shear connectors have been proposed as an alternative to welded headed studs in composite slabs with profiled steel sheeting. Unlike welded studs, bolted connectors can be easily detached, allowing steel beams to be reused rather than recycled at the end of a structure's service life [4-6].

In conventional concrete (NC) systems, many researchers have explored the performance of shear connectors through push-out tests and finite element analyses. Pavlović et al. (2013) [7] investigated the comparative behavior of headed studs and bolted connectors in normal concrete slabs and found that increasing connector height or diameter significantly enhances shear capacity and stiffness, whereas insufficient embedment may lead to brittle failure. Similarly, Arezoomand Langarudi and Ebrahimnejad (2020) [8] numerically examined composite slabs with steel decks and confirmed that connector geometry, reinforcement layout, and deck thickness influence the shear response and failure mechanisms.

In recent years, ultra-high-performance concrete (UHPC) has emerged as a promising material for next-generation composite structures due to its outstanding mechanical and durability properties [9, 10]. UHPC typically exhibits compressive strength exceeding 120 MPa, tensile strength above 10 MPa, and extremely low permeability. Its dense matrix and dispersed steel fibers provide superior stiffness, crack control, and long-term durability compared with normal concrete [11, 12]. These advantages make UHPC an attractive alternative for use in composite beams and slabs, enabling reduced self-weight, enhanced flexural rigidity, and improved service life [13-16].

A few studies have focused on shear connectors embedded in UHPC, aiming to understand their mechanical behavior and optimize design. Kim et al. (2013) [13] conducted push-out tests on headed studs in UHPC slabs and reported that UHPC

substantially increases shear strength and stiffness compared with NC, though ductility tends to decrease due to the higher modulus of elasticity. Yang et al. (2022) [17] studied studs embedded in UHPC–NSC composite slabs and found that the use of a UHPC layer around the stud root enhances both the load-bearing capacity and slip capacity while maintaining adequate ductility. Study by Li et al. [18] experimentally investigates the shear behavior of steel-UHPC composite slabs connected by epoxy resin adhesive, headed studs, and their hybrid form. Thirty-two push-out tests were conducted to evaluate failure modes, load–slip behavior, and influencing parameters. Results indicate that the hybrid connectors exhibit complex shear transfer with interface debonding and stud shrinkage. More recently, Wang et al. (2024) [19] examined the shear performance of prefabricated steel–UHPC composite beams under combined tensile and shear loading. Their results confirmed that UHPC improves the ultimate shear strength and stiffness of connectors, but the interaction of tension and shear can reduce ductility and cause mixed-mode failure at the stud root. The distinctive characteristics of UHPC necessitate a thorough re-evaluation of shear connector behavior. While UHPC generally improves the shear capacity and stiffness of conventional headed studs compared to NC [13, 17], research frequently indicates that studs embedded in UHPC often fail to meet the ductility requirement specified in design codes, such as the minimum characteristic slip of 6 mm mandated by Eurocode 4 [13, 17, 20]. These findings highlight the need for deeper investigation into the complex stress transfer mechanisms and interface behavior in steel–UHPC composite members. Despite the recent experimental progress, systematic numerical investigations on shear connectors embedded in UHPC slabs remain limited. Finite element modeling can provide a powerful tool to capture the nonlinear material behavior, interface contact, and failure evolution that are difficult to observe experimentally.

2. RESEARCH SIGNIFICANCE

The present study aims to develop a comprehensive three-dimensional nonlinear finite element model in ABAQUS to analyze the shear behavior of connectors in UHPC composite slabs with steel beams. The numerical model is validated against available test results and subsequently employed to perform a detailed parametric study considering the effects of connector diameter, concrete strength, and interface properties. The outcomes are expected to offer a better understanding of the shear transfer mechanism in steel - UHPC composite slabs and contribute to the design optimization of next-generation composite structures.

3. SIMULATION MODEL BUILD-UP

The constitutive behavior of steel, including the steel deck, steel bar and connectors, is defined using isotropic plasticity. The material response is commonly simplified using a bilinear curve [21-23]. The modulus of elasticity of steel is typically defined as 200 GPa, with a Poisson ratio of 0.3 and a density of 7850 kg/m³. The yield and ultimate strength for steel were assumed with S350 grade to be 350 and 470 MPa, respectively. To capture the failure modes, especially in shear connectors, Ductile and Shear damage models are incorporated as progressive damage models in ABAQUS [24]. The parameters for the ductile damage initiation criterion are derived based on uniaxial true plastic strain at the onset of necking.

UHPC used in this study had compressive and tensile strengths of 120 MPa and 9 MPa, respectively, with an elastic modulus of 42000 MPa. The nonlinear behavior of concrete (including UHPC) is accurately captured using the Concrete Damaged Plasticity (CDP) model in ABAQUS, recognized for its robustness in modeling reinforced concrete behavior in both static and dynamic analyses [25-28]. In ABAQUS, implementing the CDP model involves defining several essential parameters, such as the biaxial-to-uniaxial compressive strength ratio, failure surface configuration, dilation angle, eccentricity, viscosity coefficient, and the material's constitutive relationship. The specific input parameters adopted for UHPC and conventional concrete (CC) in this model are summarized in Table 1. Note that the CDP model parameters for CC are used for the numerical model validation presented in the following section.

Table 1. Parameters of the CDP model for UHPC and conventional concrete (CC)

Parameters	Value	
	UHPC [29]	CC [30]
σ_{bo}/σ_{co}	1.07	1.16
k_c	2/3	2/3
f	36^0	31^0
ϵ	0.1	0.1
Viscosity	0.005	0.005

Interaction definitions play a crucial role in accurately simulating the transfer of horizontal and vertical forces between discrete structural components, including the steel beam, steel deck, connectors, and UHPC slab. The normal contact condition was defined as hard contact, ensuring that the slave surface does not penetrate the master

surface and that no tensile stress is transmitted across the interface. The tangential contact was modeled using a penalty friction formulation with a friction coefficient (μ) of 0.4 [31, 32], which is commonly adopted for the interface between the steel deck or connectors and the concrete slab . In addition, the reinforcement cage was defined as being embedded within the concrete matrix to ensure a realistic load transfer mechanism. Boundary constraints and load applications were established to replicate the standardized push-out test configuration in accordance with Eurocode 4 specifications. To reduce computational demand, symmetry boundary conditions were applied along the relevant planes. For a half-model, displacement along the X-axis and rotations around the Y- and Z-axes were restrained (U1 = UR2 = UR3 = 0) on the symmetry plane. The loading procedure was implemented through a displacement-control method applied at the top surface of the steel beam, enabling the accurate capture of load–slip behavior during simulation. Fig. 1 presents the detailed geometry and the 3D simulation model of the bolted connectors in UHPC composite slabs with steel beams.

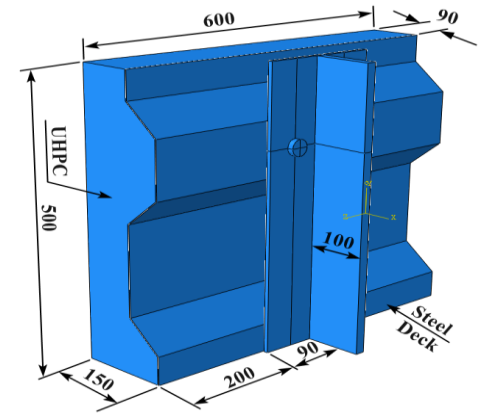

(a) Geometry

(b) 3D simulation model

Fig. 1 Bolted connectors in UHPC composite slabs with steel beams

4. RESULTS AND DISCUSSIONS

4.1 Simulation model validation

To verify the reliability and accuracy of the numerical model developed in the present study, the finite element (FE) model was validated against the experimental results reported by Rehman et al. (2016) [33] on demountable shear connectors in composite slabs with profiled steel decking. Among the test series, specimen S1 was selected as the benchmark for comparison. The experimental push-out specimen S1 consisted of two concrete slabs measuring 600 × 500 × 150 mm, cast on both sides of a 203 × 203 × 52 UB steel section. The slabs were connected to the steel beam using two shear connectors (type C1). Each connector had a shank diameter of 19 mm, a collar diameter of 17 mm. The connectors were fabricated from Grade 8.8 steel bolts, and ribbed steel bars of 10 mm diameter were used as reinforcement in a single-layer cage configuration. The profiled steel decking employed was Richard Lees Rib E60, made of S350-grade steel with a thickness of 0.9 mm. The concrete used for specimen S1 had an average cube compressive strength of 57.5 MPa. The ultimate tensile strengths of the shear connector steel and reinforcing bars were 510 MPa and 610 MPa, respectively.

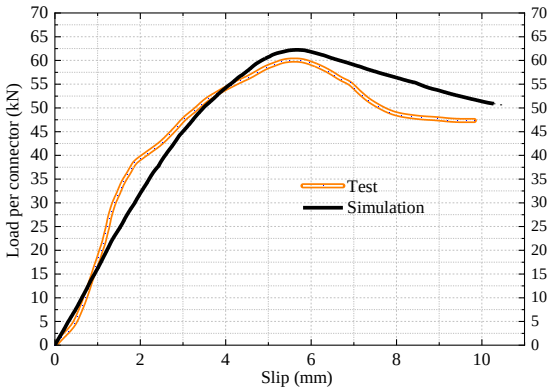

Fig. 2 Load-slip curves between push-off test specimens and simulation

Table 2. Comparison between experimental and simulation results

Case study	Maximum load per connector P_u (kN)	Slip at P_u (mm)
Test (1)	60	5.5
Simulation (2)	66.1	6.0
Disparity (2)/(1)	1.1	1.09

The comparison between the experimental and numerical load–slip responses, as illustrated in Fig. 2, demonstrates a good agreement in both the overall trend and the peak behavior. Both curves exhibit a typical nonlinear pattern characterized by an initial

linear elastic stage, followed by a nonlinear ascending branch up to the peak load, and finally a gradual descending branch due to progressive damage and slip localization at the interface. The simulation curve closely follows the experimental one throughout the loading process, accurately capturing the stiffness degradation and post-peak softening behavior. As presented in Table 2, the maximum load obtained from the simulation (66.1 kN) shows only a slight deviation of approximately 10% compared with the experimental result (60 kN). Similarly, the slip corresponding to the peak load differs marginally, with 6.0 mm for the simulation and 5.5 mm for the test. These small disparities (load ratio of 1.1 and slip ratio of 1.09) fall within an acceptable engineering tolerance, indicating that the calibrated material parameters and boundary conditions in the numerical model accurately represent the real push-out behavior.

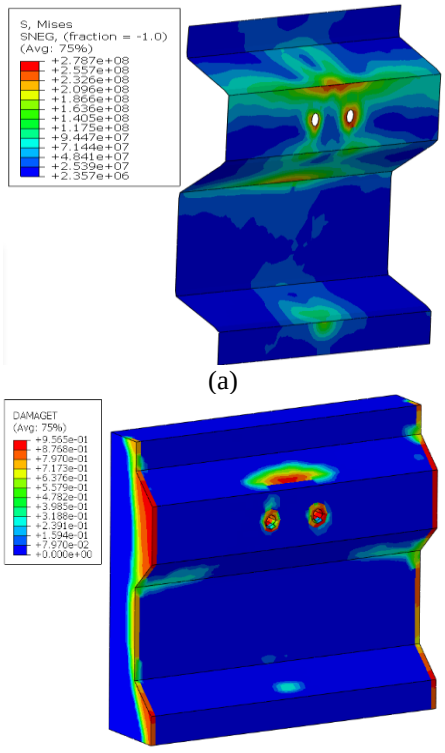

(a)

(b)

Fig. 3 Stress of steel decking (a) and damage of concrete part (b)

Fig. 3 illustrates the simulated stress distribution in the steel decking and the corresponding damage patterns in the concrete slab. The steel deck exhibits pronounced Von Mises stress concentrations around the bolt holes, indicating significant bearing action and local distortion induced by shear transfer from the bolted connectors. Elevated stress bands along the web of the steel deck further reflect localized effects, whereas the lower flange remains only lightly stressed, confirming that force transmission is highly confined to the connector region. In the concrete slab, the damage map reveals severe localized crushing and cracking immediately surrounding the bolt shanks, consistent with the high stiffness and brittle response of concrete under concentrated shear. Additional regions of moderate damage along the steel-concrete interface suggest the onset of local debonding under elevated shear demands. Importantly, damage remains confined to the connector vicinity, with no evidence of large-scale failure.

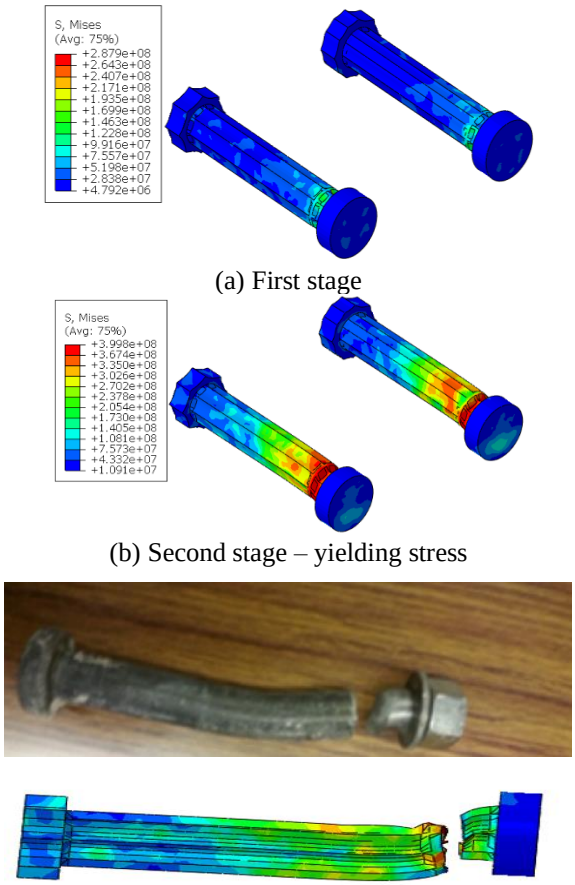

(a) First stage

(b) Second stage – yielding stress

© Final stage (Damage of the test of Rehman [33] and simulation)

Fig. 4 Damage of bolted connectors

Fig. 4 presents the progressive development of stress and damage in the bolted shear connector during loading, highlighting the transition from elastic behavior to yielding and ultimately to complete shear failure. In the first stage, the connector exhibits a predominantly elastic stress distribution, with Von Mises stresses well below the yield limit and concentrated mainly around the threaded region and the interface where shear transfer is initiated. As loading increases, the second stage reveals the onset of yielding along the bolt shank, accompanied by a significant expansion of

high-stress regions. This pattern indicates that the connector undergoes of combined shear and uplift forces in the composite system. In the final stage, both the simulation and the experimental results reported by Rehman [33] clearly show that the connector fails by shear fracture at the collar, leading to a complete separation of the bolt into two distinct pieces. The numerical model successfully captures this localized fracture mechanism, and the resulting deformation shape closely matches the experimentally observed failure.

4.2 Parametric study

After being validated through comparison with the experimental results presented above, the numerical model was further developed to perform an extended series of parametric studies. The parameters considered in this study include the compressive strength of UHPC, the diameter of the bolted shear connector, and the configuration of the reinforcement cage.

4.2.1 Effect of UHPC's compressive strength

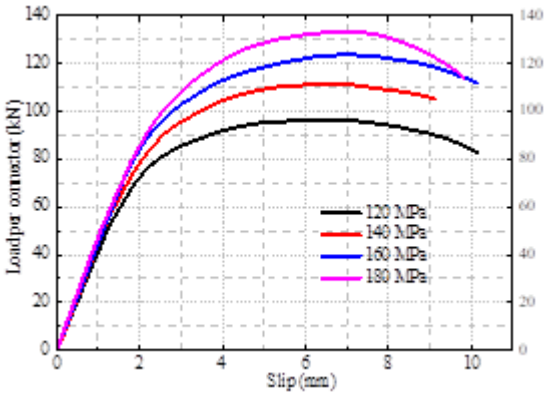

Fig. 5. Influence of UHPC compressive strength on load-slip response of bolted connectors

Table 3. Maximum load per connector under different UHPC compressive strengths

Case study	UHPC compressive strength	Maximum load per connector P_u (kN)	Increment of P_u	Note
1	120	96.8	//	//
2	140	111.3	1.15	(2)/(1)
3	160	123.5	1.11	(3)/(2)
4	180	133.4	1.08	(4)/(3)

In this parameter, the compressive strength of the UHPC was increased from 120 to 180 MPa, while all other variables, including the shear connector diameter, steel grade, geometric dimensions, etc. were kept constant. Fig. 5 and Table 3 illustrate the influence of UHPC's compressive strength on the load–slip behavior of shear connectors. The numerical results indicate a clear enhancement in the overall shear resistance and stiffness of the composite connection as the compressive strength of UHPC increases from 120 MPa to 180 MPa. At the initial loading stage, all curves exhibit a nearly linear response, representing elastic behavior of both the stud and surrounding UHPC matrix. As the load increases, the curves gradually become nonlinear due to local cracking and plastic deformation near the connector. The specimens with higher UHPC strength show a steeper ascending branch, reflecting improved confinement and bond performance between the shear connector and UHPC.

In terms of ultimate capacity, the maximum load per connector (Pu) increases from 96.8 kN for 120 MPa UHPC to 133.4 kN for 180 MPa UHPC, equivalent to an approximate 38% improvement. However, the incremental growth ratio of Pu gradually decreases (1.15→1.11→1.08), indicating that the effect of compressive strength tends to saturate beyond 160 MPa. This suggests that, after a certain threshold, further increases in matrix strength contribute less to load transfer efficiency, as failure becomes dominated by stud yielding or interface shear failure rather than UHPC crushing.

4.2.2 Effect of Shear Connector Diameter

In this parametric study, the reference case (Case 1) corresponds to a UHPC with a compressive strength of 120 MPa and a shear connector diameter of 17 mm. To evaluate the influence of connector size on the overall shear behavior, the shear connector diameter was increased successively to 19 mm, 20 mm, and 22 mm while keeping other parameters constant. The resulting load–slip relationships are presented in Fig. 6, and the corresponding maximum load capacities are summarized in Table 4. The results clearly demonstrate that increasing the connector diameter significantly enhances both the initial stiffness and ultimate load capacity of the shear connection. As the diameter increases from 17 mm to 22 mm, the peak load per connector rises from 96.8 kN to 147.3 kN, representing a total improvement of approximately 52 %. The incremental growth ratios between successive cases are 1.14, 1.18, and 1.13. This diminishing return is attributed to the nonlinear stress distribution within the UHPC matrix and the limited confinement effect beyond a certain connector size. Compared to the parameter of UHPC compressive strength, varying the connector diameter provides a more pronounced improvement in the load-carrying capacity of the composite connection, emphasizing the strong influence of mechanical interlocking and bearing action at the connector-UHPC interface. From the load–slip curves, larger-diameter shear connectors exhibit a steeper ascending branch, implying a higher stiffness and better interfacial bond between the shear

connector and UHPC. Moreover, the peak load occurs at a slightly larger slip value for bigger shear connectors, showing that increased diameter not only improves strength but also maintains a reasonable level of ductility. Conversely, smaller shear connector (17 mm) shows earlier stiffness degradation and a more gradual post-peak decline, indicating weaker anchorage and earlier onset of local concrete crushing or shear failure.

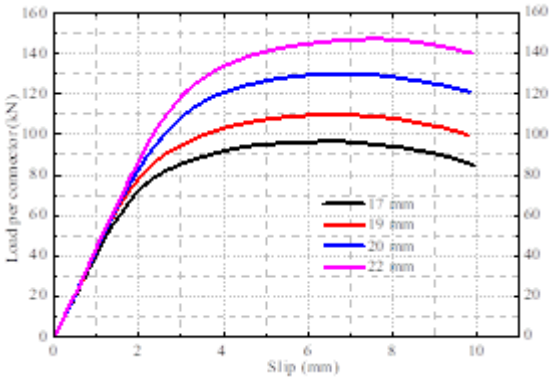

Fig. 6. Influence of diameter on load–slip response of shear connectors

Table 4. Maximum load per connector with different shear connector diameter

Case study	Shear connector diameter (mm)	Maximum load per connector P_u (kN)	Increment of P_u	Note
1	17	96.8	//	//
5	19	109.9	1.14	(5)/(1)
6	20	130.3	1.18	(6)/(5)
7	22	147.3	1.13	(7)/(6)

4.2.3 Effect of Reinforcement Cage

In this parametric investigation, the influence of the reinforcement configuration within the UHPC, specifically the use of single versus double reinforcement layers, as well as the spacing of the reinforcement mesh, is examined to assess their effects on the load-carrying performance of the joint. From Table 5 and Fig. 7a, it is evident that the use of a double reinforcement layer slightly enhances the shear capacity of the connector compared to the single-layer configuration. The maximum load per connector (P_u) increases from 96.8 kN for the single-layer case to 99.6 kN for the double-layer case, corresponding to a 3% improvement. This modest increase suggests that the addition of a second reinforcement layer leads to enhanced interaction between the steel and concrete materials. The double layer helps to distribute tensile stresses more uniformly, delaying local cracking and improving the composite action at the steel–concrete interface. However, since UHPC already exhibits very high compressive and tensile strength with limited cracking under load, the influence of an additional reinforcement layer is relatively minor in terms of total load capacity. This indicates that the dominant factor governing the connector's behavior remains the UHPC matrix and connector geometry, rather than the reinforcement quantity.

Table 5. Maximum load per connector with single layer and double layer

Case study	Reinforcement cage	Maximum load per connector P_u (kN)	Increment of P_u	Note
1	Single layer	96.8	//	//
8	Double layer	99.6	1.03	(8)/(1)

Table 6. Maximum load per connector with different spacing of reinforcement bars (Single layer of reinforcement cage)

Case study	Spacings (mm)	Maximum load per connector P_u (kN)	Increment of P_u	Note
1	100	96.8	//	//
9	80	97.7	1.01	(9)/(1)
10	60	98.9	1.02	(10)/(9)
11	40	100.4	1.02	(11)/(10)

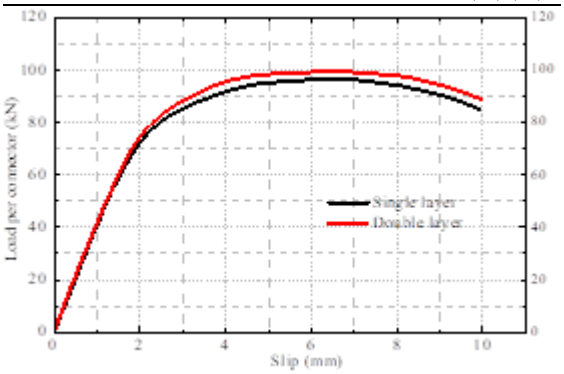

(a) Single layer and double layer

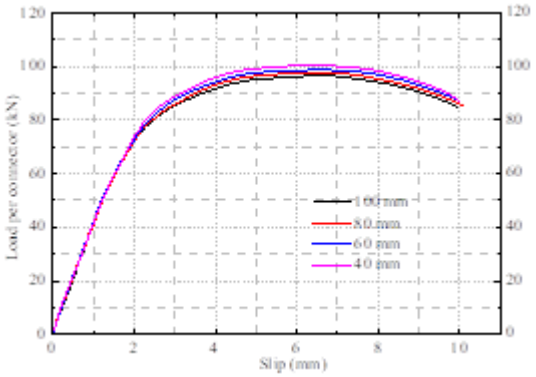

(b) Spacing of reinforcement bars

Fig. 7 Influence of reinforcement cage on load–slip response of shear connectors

In the second parametric study (Table 6 and Fig. 7b), the effect of bar spacing on the connector

performance was investigated for a single reinforcement layer with spacings of 100 mm, 80 mm, 60 mm, and 40 mm. As the spacing between reinforcement bars decreases, the maximum load per connector gradually increases, from 96.8 kN (100 mm) to 100.4 kN (40 mm). The corresponding increments of Pu are approximately 1.01 to 1.02 for each reduction step, indicating that closer reinforcement spacing provides slightly higher stiffness and load-carrying capacity. This improvement can be attributed to enhanced confinement and the reduction of local stress concentration in the UHPC, as the reinforcement grid effectively limits crack propagation and contributes to higher ductility. Nevertheless, the magnitude of increase is again modest, implying that once adequate confinement is achieved, further reduction in spacing has diminishing effects on overall performance. The load–slip curves show a similar trend for all spacing cases, maintaining a nearly identical shape, with only slight upward shifts in the peak load region. This confirms that while reinforcement spacing affects peak strength, it does not significantly alter the general failure mechanism or stiffness behavior of the connectors.

5. CONCLUSION

This study developed a comprehensive three-dimensional nonlinear finite element model to investigate the shear behavior of bolted connectors in UHPC composite slabs with steel decking. The model, constructed in ABAQUS, was validated against push-out test results. Based on the obtained results, the following conclusions can be drawn:

- Increasing the UHPC compressive strength from 120 MPa to 180 MPa resulted in significant gains in peak load and initial stiffness. However, the incremental improvement diminished at higher strength levels. Connector diameter exhibited the strongest influence among all parameters examined. Enlarging the diameter from 17 mm to 22 mm produced substantial increases in shear capacity and stiffness, highlighting the dominant role of mechanical interlocking and bearing action at the bolted connector-UHPC interface. In contrast, adjustments to the reinforcement cage, whether through adding a second layer or reducing bar spacing—yielded only marginal improvements, indicating that reinforcement primarily contributes to crack control rather than directly enhancing shear transfer.
- The validated numerical model offers a robust framework for understanding the complex interaction between UHPC and bolted connectors and can be used to support design optimization of steel-UHPC composite systems. Future research might consider cyclic loading effects, long-term degradation, and full-scale composite beam behavior to further extend the applicability of the proposed modeling approach.

6. REFERENCES

1. Guo Y.T., Chen J., Nie X. and Tao M., Investigation of the shear resistances of steel–concrete–steel composite structures with bidirectional webs. Journal of Constructional Steel Research, 2020. 164: pp. 105846.
2. Wang Y., Wang Y., Khan M., Li D. and Uy B., A review on long‐term behaviour of steel‐concrete composite structures. Proceedings in Civil Engineering, 2023. 6(3-4): pp. 268-275.
3. Yu C., Tong J.Z., Zhou S.M., Zhang J.M., State-of-the-art review on steel-concrete composite walls. Sustainable Structures, 2024. 4: pp. 1-29.
4. Fang Z., Wu J., Zhao G., Fang S. and Ma Y., Shear performance and design recommendations of single embedded nut bolted shear connectors in prefabricated steel–UHPC composite beams. Steel Compos. Struct, 2024. 50(3): pp. 319-336.
5. He J., Feng S., Vasdravellis G., Liu T., Cyclic inelastic performance evaluation of locking bolt demountable shear connectors in steel-concrete composite structures. Engineering Structures, 2024. 318: pp. 118690.
6. Luo J., Wu G., Zhao G., Ma Y. and Fang Z., Experimental and numerical analysis on shear performance of single embedded nut bolted shear connectors in prefabricated steel-UHPC composite structures under cyclic loading. Structures, 2025. 73: pp. 108446.
7. Pavlović M., Marković Z., Veljković M. and Budevac D., Bolted shear connectors vs. headed studs behaviour in push-out tests. Journal of Constructional Steel Research, 2013. 88: pp. 134-149.
8. Langarudi P.A. and Ebrahimnejad M., Numerical study of the behavior of bolted shear connectors in composite slabs with steel deck. Structures, 2020. 26: pp. 501-515.
9. Dahish H.A. and Bakri M., Flexural Behavior of Rc Composite Beams With Ultrahigh Performance Fiber Reinforced Concrete Layer Using Finite Element Modeling. International Journal of GEOMATE, 2022. 22(93): pp. 75-82.
10. Mai V.C., Nguyen T and Vu Q.A, Experimental Investigation of the Hydraulic Abrasion Resistance of Ultra High Performance Concrete under Sediment-Laden Flow. Case Studies in Construction Materials, 2025: pp. e05307.
11. Arabani A.S., Naserabadi H.D. and Aminyavari S., Experimental investigation of energy absorption in fiber-reinforced ultra high-performance concrete after exposure to elevated temperatures. Case Studies in Construction Materials, 2025. 22: pp. e04451.

12. Tran T.H., Vu Q.A. and Mai V.C., Comprehensive evaluation of flexural capacity calculation methods for ultra high performance concrete girders: experiments, simulations, and standards. International Journal of GEOMATE, 2025. 28(129): pp. 76-83.
13. Kim J.S., Park S.H., Joh C.B., Kwark J.D and Choi E.S., Push-out test on shear connectors embedded in UHPC. Applied Mechanics and Materials, 2013. 351: pp. 50-54.
14. Kravanja G., Mumtaz A.R. and Kravanja S., A comprehensive review of the advances, manufacturing, properties, innovations, environmental impact and applications of Ultra-High-Performance Concrete (UHPC). Buildings, 2024. 14(2): pp. 382.
15. Wakjira T.G. and Alam M.S., Performance-based seismic design of Ultra-High-Performance Concrete (UHPC) bridge columns with design example–Powered by explainable machine learning model. Engineering Structures, 2024. 314: pp. 118346.
16. Yang B., Zhang Y., Zhang W. and Sun H., Recycling lithium slag into eco-friendly ultra-high performance concrete: Hydration process, microstructure development, and environmental benefits. Journal of Building Engineering, 2024. 91: pp. 109563.
17. Yang H., Zheng Y., Mo S. and Lin P., Push-out tests on studs with UHPC cover embedded in UHPC-NSC composite slab. Construction and Building Materials, 2022. 331: pp. 127210.
18. Li C., Chen B., Hu W. and Sennah K., Push-out test of hybrid shear connector in steel-precast UHPC composite slab. Structures, 2023. 50: pp. 1767-1782.
19. Wang G., Xian B., Ma F. and Fang S., Shear performance of prefabricated steel Ultra-High-Performance Concrete (UHPC) composite beams under combined tensile and shear loads: single embedded nut bolts vs. studs. Buildings, 2024. 14(8): pp. 2425.
20. Standardization, E.C.f., Eurocode 4: Design of composite steel and concrete structures. 2004. pp. 1998-1.
21. Akbari J., Rozbahani S. and Isari M., Effect of moving resonance on the seismic responses under far-field and near-field earthquakes. Asian Journal of Civil Engineering, 2021. 22(1): pp. 159-173.
22. Ayough P., Ibrahim Z., Jameel M. and Alnahhal A., Axial compression behaviour of circular concrete-filled double-skin steel tubular columns with bolted shear studs: Numerical investigation and design. Journal of Constructional Steel Research, 2023. 205: pp. 107911.
23. Vu Q.A. and Mai V.C., Estimating the Punching Shear Capacity of Voided Reinforced Concrete Slab. International Journal of GEOMATE, 2024. 27(124): pp. 128-135.
24. Systèmes, D., Abaqus/CAE User's Guide. 2016.
25. Chen M., Mingzhu C., Wouter D.C., Fan Z. and Luc T., Parametric Analysis of CDP Modeling of High-Strength Concrete in Abaqus to Study the Direct-Shear Behavior of Joints in Precast Concrete Segmental Bridges. in International Conference on Engineering Structures. Springer. 2024: pp. 318-328.
26. Annapoorna C.H. and Appa Rao G., Calibration of Concrete Damage Plasticity (CDP) Parameters for Numerical Analysis of Reinforced Concrete Structure. in International Colloquium on Performance, Protection & Strengthening of Structures Under Extreme Loading & Events. Springer. 2024. pp. 1-519.
27. Mohammed I., Zhou Z. and Ai C., Stress and damage assessment in concrete pavement surrounding dowels: a CDP model approach. International Journal of Pavement Engineering, 2025. 26(1): pp. 2486486.
28. Yao Z., Zhou J., Chang X. and Cui T., Plastic performance of recycled concrete based on ABAQUS. in 13th Annual International Conference on Material Science and Environmental Engineering (MSEE 2025). 2025. SPIE. pp. 1-7.
29. Bahij S., Adekunle S.K, Al‐Osta M., Ahmad S. and Al‐Dulaijan S.U., Numerical investigation of the shear behavior of reinforced ultra‐high‐performance concrete beams. Structural Concrete, 2018. 19(1): pp. 305-317.
30. Hafezolghorani M., Hejazi F., Vaghei R., Jaafar M. and Karimzade K., Simplified damage plasticity model for concrete. Structural engineering international, 2017. 27(1): pp. 68-78.
31. Guo Q., Chen Q., Xing Y., Xu Y. and Zhu Y., Experimental Study of Friction Resistance between Steel and Concrete in Prefabricated Composite Beam with High‐Strength Frictional Bolt. Advances in Materials science and Engineering, 2020 (1): pp. 1292513.
32. Rinker M., Pilli S.P. and Karri N.K., Structural Integrity of Single Shell Tanks at Hanford. WM2009 Conference, March 1-5, 2009: pp. 1-9
33. Rehman N., Lam D., Dai X. and Ashour A.F., Experimental study on demountable shear connectors in composite slabs with profiled decking. Journal of Constructional Steel Research, 2016. 122: pp. 178-189.